Different initiation of pre-TCR and γδTCR signalling

Claude Saint-Ruf, Maddalena Panigada, Orly Azogui, Pascale Debey, Harald von Boehmer, Fabio Grassi

....

Different initiation of pre-TCR and γδTCR signalling

Claude Saint-Ruf*, **Maddalena Panigada**†, **Orly Azogui***, **Pascale Debey**‡, **Harald von Boehmer**§ & **Fabio Grassi***†

* *Institut Necker, U INSERM 373, Faculté de Médecine Necker, 156 Rue de Vaugirard, F75730, Paris cedex 15, France*
† *Unité INRA 806, Muséum National d'Histoire Naturelle, Institut de Biologie Physico-Chimique, 13, Rue Pierre et Marie Curie, 75005 Paris, France*
‡ *Dipartimento di Biologia e Genetica per le Scienze Mediche, Università degli Studi di Milano, Via Viotti 3/5, 20133 Milano, Italy*
§ *Harvard Medical School, Dana-Farber Cancer Institute, 44 Binney Street, Smith 736, Boston, Massachussetts, 02115, USA*

....

Lineage choice is of great interest in developmental biology. In the immune system, the αβ and γδ lineages of T lymphocytes diverge during the course of the β-, γ- and δ-chain rearrangement of T-cell receptor (TCR) genes that takes place within the same precursor cell and which results in the formation of the γδTCR or pre-TCR proteins[1–3]. The pre-TCR consists of the TCRβ chain covalently linked to the pre-TCRα protein, which is present in immature but not in mature T cells which instead express the TCRα chain[4,5]. Animals deficient in pre-TCRα have few αβ lineage cells but an increased number of γδ T cells. These γδ T cells exhibit more extensive TCRβ rearrangement than γδ T cells from wild-type mice[6,7]. These observations are consistent with the idea that different signals emanating from the γδTCR and pre-TCR instruct lineage commitment[8]. Here we show, by using confocal microscopy and biochemistry to analyse the initiation of signalling, that the pre-TCR but not the γδTCR colocalizes with the p56[lck] Src kinase into glycolipid-enriched membrane domains (rafts) apparently without any need for ligation. This results in the phosphorylation of CD3ε and Zap-70 signal transducing molecules. The results indicate clear differences between pre-TCR and γδTCR signalling.

The analysis by confocal microscopy of pre-TCRα (pTα) distribution in the plasma membrane of pre-TCR expressing thymocytes revealed a punctate staining pattern in contrast to the more diffuse and uniform distribution of CD25 (Fig. 1Aa–c). Peripheral αβ T cells and γδ thymocytes also exhibited a more uniform receptor staining (Fig. 1Ad–g). Quantitation of colocalization of pTα and TCRβ chains on the surface of thymocytes revealed a strong positive correlation[9] (correlation coefficient 0.95) and therefore the almost complete colocalization of the long pTα isoform with the TCRβ chain in patches of the cell membrane from immature thymocytes (Fig. 1Ba–e). The patchy distribution of the pre-TCR was reminiscent of the distribution on the cell surface of the αβTCR after ligand binding[10], which is caused by crosslinking of the αβTCR and subsequent localization into glycolipid-enriched membrane domains (rafts)[11–14]. These rafts contain GPI-linked proteins, Src-like tyrosine kinases and other proteins targeted to rafts through saturated acyl chains[15–18]. As the patchy distribution of the pre-TCR could conceivably be due to localization into rafts, we tested whether the pre-TCR, in the absence of any deliberate ligation, would colocalize with raft components in the membrane

of a SCID thymocyte-derived cell line (SCIET.27) that had been transfected with a productive TCRβ gene and expressed the pre-TCR on the cell surface (SCB.29)[4]. Co-staining with GM$_1$-binding cholera toxin B (CTxB) and pTα antibodies revealed the same clustered distribution of the pre-TCR as observed with thymocytes and colocalization with GM$_1$ (Fig. 2Aa–d). A similar colocalization was also observed with thymocytes (data not shown). These results suggested that a putative pre-TCR ligand on thymic stroma was not essential for the patchy staining and colocalization with GM$_1$.

The pre-TCR clustering was significantly reduced after cholesterol depletion with methyl-β-cyclodextrin (MβCD) (Fig. 2Ae, f), indicating the requirement for an intact lipid configuration. This suggests that the observed staining pattern was not caused by antibody crosslinking, because lateral mobility of transmembrane proteins is not inhibited by cholesterol depletion[19]. We also transfected the SCIET.27 cell line with a vector encoding a (Vβ8.2Dβ1Jβ2.6Cβ2) TCRβ chain–enhanced green fluorescent (eGFP) fusion protein and found a clustered distribution of the tagged pre-TCR by confocal microscopy. No such clustering occurred with GFP protein alone (Fig. 2Ba–d). This further ruled out a requirement for pre-TCR crosslinking. (The large area of intracellular staining in Fig. 2Bc may represent internalized receptors).

To assess whether expression of a γδTCR would yield a similarly patchy staining, we transfected Vγ1Jγ1Cγ4 and Vδ7.1Jδ1Cδ genes into the same pro-T cell line SCIET.27. Even though the γδTCR was expressed at similar levels, the staining was much more homogenous (Fig. 2Be, f).

Genetic evidence implicates p56[lck] as an essential component in pre-TCR function[20]. We therefore tested whether the pre-TCR would colocalize with p56[lck] in roughly the same way that it colocalizes with the αβTCR after crosslinking[21–23]. We found that
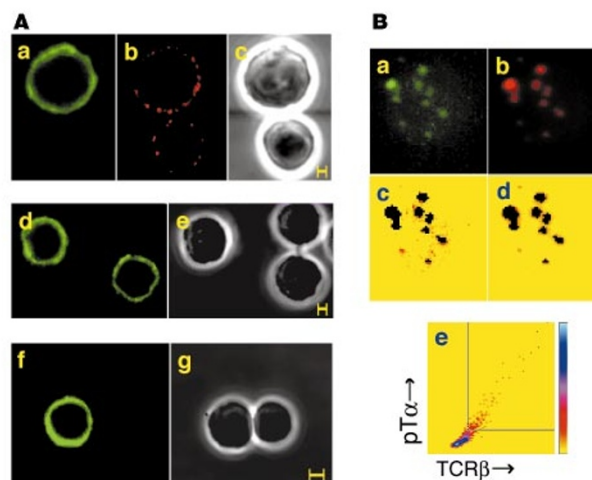

Figure 1 Analysis of the pre-TCR in the cell membrane of thymocytes. **A**, Punctate pattern of pTα chains on the surface of CD4⁻8⁻ thymocytes. Co-staining of CD4⁻8⁻ thymocytes with FITC-conjugated PC-61 (anti-CD25) monoclonal antibody (**a**) and biotinylated 2F5 (anti-pTα) monoclonal antibody revealed by streptavidin–TR (**b**), with phase contrast image (**c**). Staining of γδ thymocytes with biotin-labelled GL-3 monoclonal antibody revealed by streptavidin–FITC (**d**, **e**). Staining of lymph nodes cells with FITC-conjugated H57-597 monoclonal antibody (**f**, **g**). Scale bar, 2 μm. **B**, Quantitative colocalization analysis of TCRβ and full-length pTα chains on the surface of CD4⁻8⁻ thymocytes. Cells were stained with FITC-conjugated H57-597 (anti-TCRβ) and biotin-labelled 2F5 (anti-pTα) monclonal antibodies revealed by streptavidin–TR. Spatial distribution of TCRβ (**a**) and pTα (**b**) stainings and corresponding SPIMAC 2D histogram (**e**). Areas outside the selected region in the 2D histogram represent the background; the pixels comprised in the region appear in black in the TCRβ (**c**) and pTα (**d**) images and correspond to the green and red dots in **a** and **b**.

more than 80% of the pTα signals colocalized with p56^{lck} signals (correlation coefficient 0.85; Fig. 2Ca−e). The same analysis performed with pTα- and CD25-dependent fluorescence shows that pTα signals cannot be integrated into a homogeneous subset with respect to CD25 signals and that there is only occasional colocalization by chance (correlation coefficient 0.47; Fig. 2Cf−l).

The observed spontaneous colocalization of pre-TCR and p56^{lck} kinase in rafts might bring the pre-TCR-associated CD3ϵ and CD3ζ chains into contact with p56^{lck}, resulting in cell-autonomous activation of proximal signalling, that is, phosphorylation of CD3ϵ and CD3ζ chains as well as Zap-70. We tested this by directly analysing the colocalization biochemically, and by determining CD3 and Zap-70 phosphorylation in the pre-TCR competent (SCB.29) and pre-TCR incompetent (SCIET.27) cell lines. Immunoblot analysis with
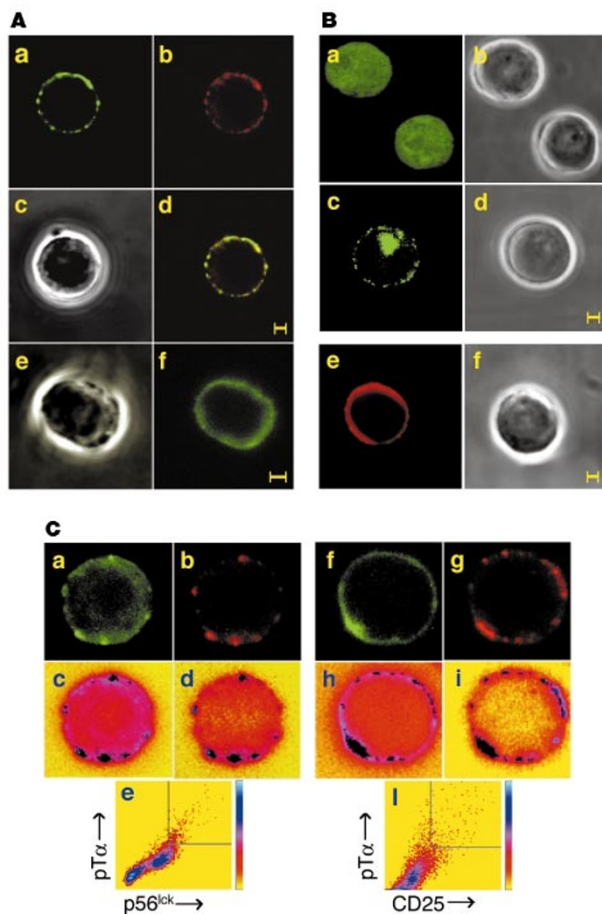

Figure 2 Analysis of the pre-TCR in the cell membrane of SCB.29 cells. **A**, Colocalization of GM$_1$ with pTα chains on the surface of SCB.29 cells by confocal microscopy. Cells were stained with FITC-labelled CTxB monoclonal antibody (**a**) and biotinylated 2F5 monoclonal antibody revealed by streptavidin−TR (**b**); phase contrast (**c**) and merged (**d**) images are shown. By quantitative colocalization analysis, 77% of pTα staining colocalizes with CTxB. Staining of SCB.29 cells treated with MβCD with biotinylated 2F5 monoclonal antibody revealed by streptavidin−FITC (**e**, **f**). Scale bar, 2 μm. **B**, Analysis by confocal microscopy of SCIET.27 cells expressing eGFP (**a**, **b**) and TCRβ−eGFP (**c**, **d**). Staining of SCIET.27 cells expressing $\gamma\delta$TCR with biotin-labelled 3A10 (anti-TCRδ) monoclonal antibody revealed by streptavidin−TR (**e**, **f**). Scale bar, 2 μm. **C**, Quantitative colocalization analysis of pTα chains and p56^{lck} in SCB.29 cells. Cells were stained with anti-Lck monoclonal antibody revealed by FITC-labelled goat anti-mouse Ig (**a**) and rabbit anti-pTα Ig revealed by TR-conjugated goat anti-rabbit Ig (**b**); the corresponding SPIMAC 2D histogram is shown (**e**). Areas outside the selected region in the histogram represent the background. The selected region is depicted in black in the p56^{lck} (**c**) and pTα (**d**) images. As a control, cells were stained with FITC-conjugated PC-61 (anti-CD25) monoclonal antibody (**f**) and rabbit anti-pTα Ig revealed by TR-conjugated goat anti-rabbit Ig (**g**).
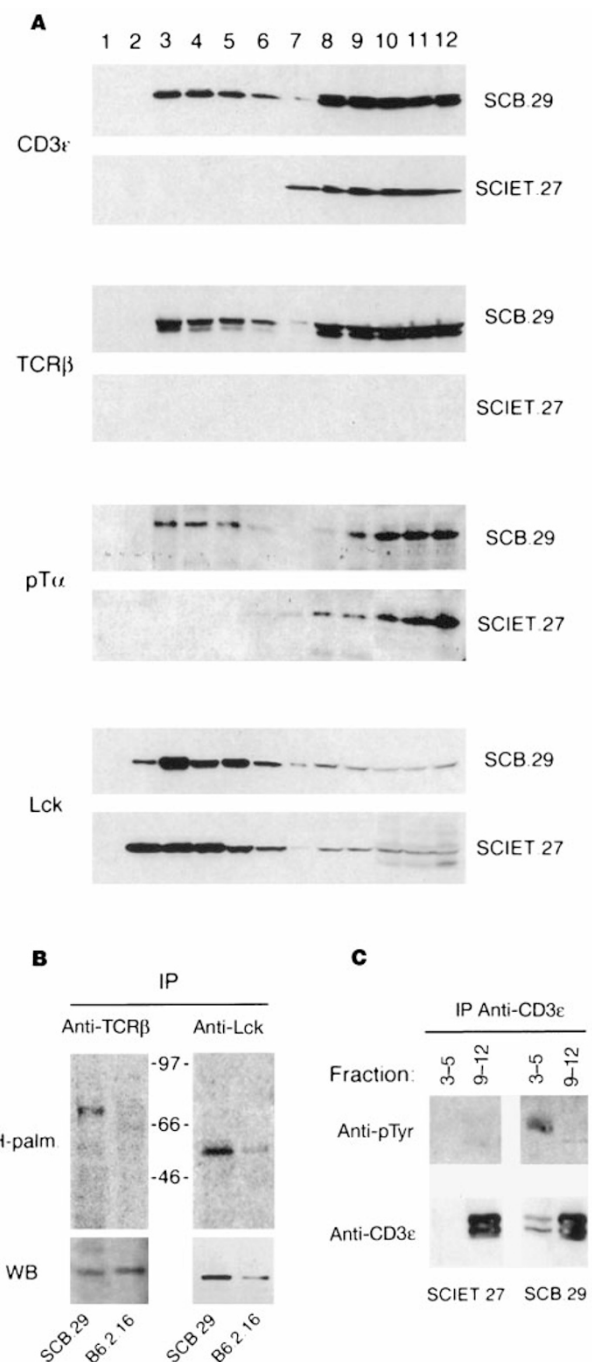

Figure 3 Biochemical analysis of the pre-TCR. **A**, Partition of pre-TCR into rafts analysed by sucrose gradient fractionation. Western blot with the indicated antibodies of TCA-precipitated sucrose gradient fractions from SCB.29 and SCIET.27 cell lysates. The analysis with the different antibodies was performed on the same membranes for both SCB.29 and SCIET.27 cell lysates. **B**, Palmitoylation of pTα chain. Lysates from biosynthetically labelled cells with ^{3}H-palmitate were immunoprecipitated either with anti-TCRβ or anti-Lck monoclonal antibodies. After separation in non-reducing gels, the immunoprecipitates were transferred onto nitrocellulose membranes. Autoradiographies (4-week exposure) and corresponding western blot with F23.1 and anti-Lck monoclonal antibodies are shown. **C**, CD3ϵ phosphorylation in raft fractions of SCB.29 cells. Anti-CD3ϵ immunoprecipitates of the indicated fractions from sucrose gradients were resolved in non-reducing gels, transferred to nitrocellulose membranes and sequentially probed with anti-phosphotyrosine (4G10) and anti-CD3ϵ antibodies. In non-reducing conditions, CD3ϵ chains migrate as a doublet and tyrosine phosphorylation is confined to the upper band.

525

specific antibodies of sucrose gradient fractions containing Triton X-100 SCB.29 and SCIET.27 cell lysates revealed the presence of pTα and CD3ε chains in low-density fractions in SCB.29 but not SCIET.27 cells (Fig. 3A). In contrast, p56[lck] was found in low-density fractions of both cells owing to its spontaneous localization into rafts[16,17]. The recovery of TCRβ, pTα and CD3ε proteins from low-density fractions was abolished by treatment with MβCD before the lysis of cells (data not shown).

These biochemical results show independently that the pre-TCR localizes cell-autonomously into rafts. Such localization could possibly be mediated by the palmitoylation of the juxtamembraneous cysteine residue conserved in both the human and the murine pTα protein[24]. We therefore used metabolic labelling with ³H-palmitate, followed by immunoprecipitation with TCRβ antibodies from cell lysates of SCB.29 and the B6.2.16 hybridoma (which expressed the same TCRβ chain as SCB.29, but in covalent linkage with the TCRα chain). Whereas we did not detect labelled αβTCR, we observed incorporation of ³H-palmitate into the pre-TCR in the SCB.29 cells (Fig. 3B). The ability to abolish the label with hydroxylamine confirmed the linkage of the ³H-palmitate label to the protein. The palmitoylated band corresponding to the pre-TCR was detected also when immunoprecipitations were carried out with anti-pTα and anti-CD3ε antibodies (data not shown).

The recovery of phosphorylated CD3ε chains from low-density fractions of cell lysates from SCB.29 but not SCIET.27 cells (Fig. 3C) suggested a functional significance of pre-TCR and p56[lck] colocalization in rafts. Previously, weakly phosphorylated ζ-chains were found to coprecipitate with Zap-70 in unstimulated SCB.29 cells,

suggesting activation of Zap-70 (ref. 25). Zap-70 is recruited and activated by phosphorylated CD3ε (ref. 26). We therefore analysed whether phosphorylated Zap-70 could be recovered from both particulate and soluble fractions of SCB.29 cells but not SCIET.27 cells (Fig. 4A). Phosphorylation was detected in SCIET.27 cells that were independently transfected with five different TCRβ genes (Vβ8.2 Dβ1Jβ2.6Cβ2, Vβ8.2 Dβ2 Jβ2.6Cβ2, two Vβ12 Jβ2.6Cβ2 with different CDR3 regions, and Vβ4Jβ2.6Cβ2) (data not shown), but not in non-transfected cells. This effectively eliminates the possibility that phosphorylation was due to the selection of a rare variant in culture and/or being dependent on a particular TCRβ/pTα combination. Disruption of raft integrity by MβCD or inhibition of p56[lck] by the specific inhibitor PP2 resulted in complete loss of Zap-70 phosphorylation (Fig. 4A). The phosphorylation in SCB.29 cells was unlikely to be caused merely by elevated levels of CD3 and Zap-70 after expression of the pre-TCR: whereas particular γδTCR and TCRβ transfectants of SCIET.27 exhibited the same CD3ε expression on the cell surface by cytometry, phosphorylated Zap-70 was detected in TCRβ but not TCRγδ transfectants (Fig. 4B), even though Zap-70 was detected at comparable levels in the γδTCR-expressing cell lines by immunoblotting and was targeted to the plasma membrane independently of its phosphorylation, as previously described[27] (Fig. 4B).

Thus, a fundamental difference exists in the manner by which the γδTCR and the pre-TCR initiate signal transduction. Our data indicate that the pre-TCRα protein may have specifically evolved to pair with the TCRβ chain and to segregate cell-autonomously into rafts as do other palmitoylated proteins. This sequestration into rafts apparently suffices to initiate the pre-TCR signalling. Such signalling may or may not involve binding of the pre-TCR to a ligand expressed by pre-T cells themselves. However, data obtained with a truncated pre-TCR may suggest that binding to the extracellular portion of the pre-TCR is not required[28]. Differences in pre-TCR and γδTCR signalling may instruct immature T cells to develop along different pathways.   □
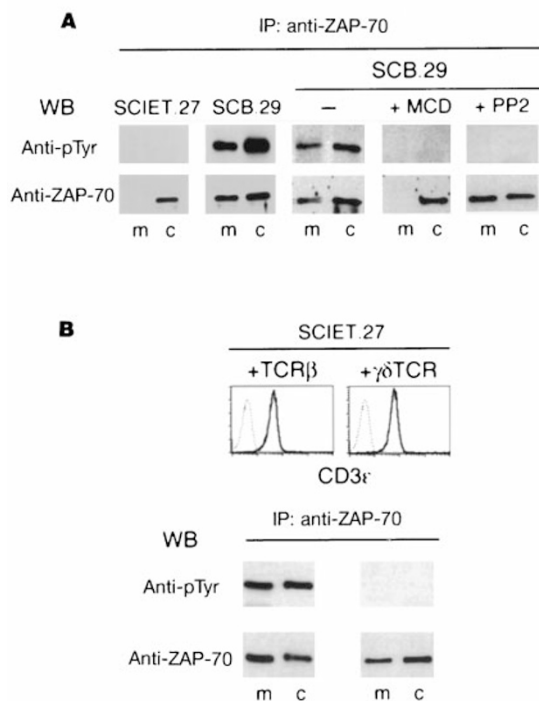

Figure 4 Cell-autonomous pre-TCR signalling in rafts. **A**, Constitutive phosphorylation of ZAP-70 in SCB.29 cells, and dependence on raft integrity and p56[lck] activity. Membrane (m) and cytosol (c) fractions from SCIET.27 and SCB.29 cells were immunoprecipitated with anti-ZAP-70 antibodies and analysed with anti-phosphotyrosine (4G10) monoclonal antibody and anti-ZAP-70 rabbit Ig; the same analysis on untreated and MβCD- and PP2-treated SCB.29 cells is shown. **B**, Lack of constitutive ZAP-70 phosphorylation by γδTCR expression in SCIET.27 cells. Flow cytometry of two clones from TCRβ and γδTCR transfections of SCIET.27 cells stained with biotin-labelled 145-2C11 (anti-CD3ε) monoclonal antibody revealed by streptavidin–PE. The same two clones were analysed for ZAP-70 phosphorylation in both membrane (m) and cytosol (c) fractions.

Methods

Antibodies and expression vectors

We used the following antibodies: FITC-conjugated anti-TCRβ (H57-597) and anti-CD25 (PC-61) monoclonal antibodies (Pharmingen); biotin-conjugated anti-pTα (2F5)[7], anti-TCRδ (3A10), anti-CD3ε (145.2C11) and anti-TCRγδ (GL-3) (Pharmingen) monoclonal antibodies; unlabelled anti-CD4 (RL1.72), anti-CD8 (31LM), anti-CD3((145.2C11) and anti-Vβ8 (F23.1) monoclonal antibodies purified from culture supernatants; anti-Lck (MOL171) (Pharmingen) and anti-phosphotyrosine (4G10) monoclonal antibody (Upstate Biotechnology); rabbit anti-pTα[7], anti-Lck, anti-ZAP-70 and goat anti-CD3ε immunoglobulins (Ig) (Santa Cruz). We used the following secondary reagents: streptavidin-labelled with FITC, phycoerythrin (PE), Texas red (TR) (Southern Biotechnology) and horseradish peroxidase (HRP) (Amersham), TR-conjugated goat anti-rabbit and FITC-conjugated goat anti-mouse Ig (Southern Biotechnology), sheep anti-mouse, donkey anti-rabbit (Amersham) and rabbit anti-goat (Valbiotech) Ig labelled with HRP. For the generation of SCIET.27 cells expressing the pre-TCR tagged with enhanced green fluorescent protein (eGFP), full-length cDNA of the TCRβ gene Vβ8.2Dβ1Jβ2.6Cβ2 was cloned in peGFP-N1 vector (Clontech) to express TCRβ fused to the amino terminus of eGFP. For transfection of SCIET.27 cells with TCRβ, rearranged TCRβ DNAs were cloned into pHb Apr-1-neo vector[29], whereas for expression of TCRγδ, SCIET.27 cells were co-transfected with TCRγ and TCRδ genes derived from cDNA of TCRγδ transgenic thymocytes and cloned into pHb Apr-1-neo and pSVL (Pharmacia) plasmids, respectively. SCIET.27 cells were transfected by electroporation, and surface expressions of the pre-TCR or TCRγδ on resistant clones were checked in flow cytometry with appropriate monoclonal antibodies.

Fluorescence microscopy and image analysis

Double negative CD4⁻8⁻ thymocytes expressing the pre-TCR were highly enriched from thymi of 3–4-week-old C57BL/6 TCRα⁻/⁻ mice by complement-mediated depletion of CD4 and CD8 expressing thymocytes followed by selection at the cell sorter of cells negative for DX 5 (NK cells) and γδTCR expression. For staining of γδ thymocytes, the same procedure was followed with exclusion of the anti-γδTCR monoclonal antibody during sample preparation for cell sorting. Peripheral lymph node T cells were enriched from lymph nodes by Dynabead (Dynal) depletion of IgM⁺ B cells. The SCIET.27 and SCB.29 cell lines have been described[4]. After adhesion on poly-L-lysine coated coverslip, the cells were fixed in paraformaldehyde and incubated on ice for 45 min with antibodies in PBS, 3% fetal calf serum (FCS) and sodium azide. For staining of the gangliosides GM₁,

FITC-labelled cholera toxin B (CTxB) subunit (Sigma) was used in the absence of FCS. When required, washed cells were stained with the specific second step reagent.

For intracellular staining, fixed cells were labelled with anti-pTα antibodies and permeabilized in PBS with 0.15% Triton X-100 for 5 min followed by staining with anti-p56[lck] antibodies. Cells were depleted of membrane cholesterol by treatment with 10 mM methyl-β-cyclodextrin (Sigma) in Dulbecco's modified Eagle's medium supplemented with 0.4% fatty-acid-free bovine serum albumin, 1 µg ml^{-1} transferrin, 8.1 µg ml^{-1} monothioglycerol and 20 mM HEPES pH 7.4 (lipid-free medium) for 1 h at 37 °C. Confocal microscopy was done on a LSM 510 Zeiss confocal microscope. For quantitative colocalization analysis, we used a Zeiss inverted microscope (Axiovert 35) as conventional microscopy is more sensitive than confocal microscopy for this analysis[9]. Images were acquired and processed with a CCD camera (Photometrics) cooled to 10 °C and coupled to the IPLAB Spectrum Imaging software. The spatial distribution of two labelled molecules was analysed on recorded images using the Co-localization Image Analysis program from the SPIMAC (Spectral Imaging on Macintosh) software as described[9].

Subcellular fractionations, biosynthetic labelling and western blotting

Cells were lysed in Triton X-100 as described[12], mixed with 1 ml 80% sucrose, and overlaid with two phases of 2 ml 30% sucrose and 1 ml 5% sucrose, respectively. Samples were centrifuged at 200,000g at 4 °C for 14–16 h, and 0.4 ml fractions were collected and numbered from the top of the gradient, precipitated in trichloroacetic acid (TCA), resolved by SDS–PAGE in reducing 8–15% gradient gels, transferred to nitrocellulose membranes and blotted with the indicated antibodies and specific secondary reagents. For analysis of CD3ε phosphorylation, raft fractions (from 3 to 5) and loading zone fractions (from 9 to 12) were immunoprecipitated with anti-CD3ε monoclonal antibody followed by Protein A Sepharose. Anti-CD3ε immunoprecipitates were resolved by SDS–PAGE in non-reducing 8–15% gradient gels, transferred to nitrocellulose membranes and sequentially blotted with anti-phosphotyrosine mAb 4G10 and goat anti-CD3ε Ig.

Biosynthetic labelling of endogenous palmitate was carried out by incubation of cells in the presence of ^{3}H-palmitate (0.5 mCi) for 4 h at 37 °C in lipid-free medium without monothioglycerol. Cells were lysed in 1% Triton X-100, 0.2% saponin, and lysates were immunoprecipitated with either anti-TCRβ or anti-Lck monoclonal antibody coupled to Protein A Sepharose. After separation by SDS–PAGE in non-reducing conditions, samples were transferred to nitrocellulose membranes, which were used for autoradiography with BioMax TranScreen intensifying system (Kodak). For membrane and cytosol separation, either untreated cells or cells treated with 10 mM MβCD or 10 µM PP2 (Calbiochem) for 15 min at 37 °C, were lysed in hypotonic buffer (20 mM Tris-HCl pH 7.5, 1 mM EGTA, 1 mM MgCl$_2$, 0.5 mM DTT and protease inhibitors) and disrupted by homogenization on ice with a Dounce homogenizer. Salt concentration was adjusted to 150 mM NaCl, and intact cells, nuclei and cytoskeleton were pelleted by two centifugations at 5,000 r.p.m. for 5 min in microcentrifuge at 4 °C. The supernatant was centrifuged at 100,000g for 1 h and membrane pellets solubilized in 0.5% Triton X-100 for immunoprecipitation with anti-ZAP-70 Ig. The supernatant corresponding to cytosol was equilibrated to 0.5% Triton X-100 and immunoprecipitated with anti-ZAP-70 Ig.

1. von Boehmer, H. & Fehling, H. J. Structure and function of the pre-T cell receptor. *Annu. Rev. Immunol.* **15**, 433–452 (1997).
2. Godfrey, D. I., Kennedy, J., Suda, T. & Zlotnik, A. A developmental pathway involving four phenotypically and functionally distinct subsets of CD3⁻CD4⁻CD8⁻ triple negative adult mouse thymocytes defined by CD44 and CD25 expression. *J. Immunol.* **150**, 4244–4252 (1993).
3. Rodewald, H. R. *et al.* FcγRII/III and CD2 expression mark distinct subpopulations of immature CD4⁻8⁻ murine thymocytes: In vivo developmental kinetics and T cell receptor β chain rearrangement status. *J. Exp. Med.* **177**, 1079–1092 (1992).
4. Groettrup, M. *et al.* A novel disulfide-linked heterodimer on pre-T cells consists of the T cell receptor β chain and a 33 kd glycoprotein. *Cell* **75**, 283–294 (1993).
5. Saint-Ruf, C. *et al.* Analysis and expression of a cloned pre-T cell receptor gene. *Science* **266**, 1208–1212 (1994).
6. Fehling, H. J., Krotkova, A., Saint-Ruf, C. & von Boehmer, H. Crucial role of the pre-T-cell receptor α gene in development of αβ but not γδ T cells. *Nature* **375**, 795–798 (1995).
7. Aifantis, I. *et al.* On the role of the pre-T cell receptor in αβ versus γδ lineage commitment. *Immunity* **9**, 649–655 (1998).
8. von Boehmer, H. *et al.* Crucial function of the pre-T cell receptor (TCR) in TCRβ selection, TCRβ allelic exclusion and αβ versus γδ lineage commitment. *Immunol. Rev.* **165**, 111–119 (1998).
9. Amirand, C. *et al.* Three distinct sub-nuclear populations of HMG-I protein of different properties revealed by co-localization image analysis. *J. Cell Sci.* **111**, 3551–3561 (1998).
10. Janes, P. W., Ley, S. C. & Magee, A. I. Aggregation of lipid rafts accompanies signaling via the T cell antigen receptor. *J. Cell Biol.* **147**, 447–461 (1999).
11. Xavier, R., Brennan, T., Li, Q., McCormack, C. & Seed, B. Membrane compartmentation is required for efficient T cell activation. *Immunity* **8**, 723–732 (1998).
12. Montixi, C. *et al.* Engagement of T cell receptor triggers its recruitment to low-density detergent-insoluble membrane domains. *EMBO J.* **17**, 5334–5348 (1998).
13. Simons, K. & Ikonen, E. Functional rafts in cell membranes. *Nature* **387**, 569–572 (1997).
14. Harder, T., Scheiffele, P., Verkade, P. & Simons, K. Lipid domain structure of the plasma membrane revealed by patching of membrane components. *J. Cell Biol.* **141**, 929–942 (1998).
15. Brown, D. A. & Rose, J. K. Sorting of GPI-anchored proteins to glycolipid-enriched membrane subdomains during transport to the apical cell surface. *Cell* **68**, 533–544 (1992).
16. Shenoy-Scaria, A. M., Dietzen, D. J., Kwong, J., Link, D. C. & Lublin, D. M. Cysteine 3 of Src family protein tyrosine kinase determines palmitoylation and localization in caveolae. *J. Cell Biol.* **126**, 353–363 (1994).
17. Rodgers, W., Crise, B. & Rose, J. K. Signals determining protein tyrosine kinase and glycosyl-phosphatidylinositol-anchored protein targeting to a glycolipid-enriched membrane fraction. *Mol. Cell. Biol.* **14**, 5384–5391 (1994).
18. Zhang, W., Trible, R. P. & Samelson, L. E. LAT palmitoylation: its essential role in membrane microdomain targeting and tyrosine phosphorylation during T cell activation. *Immunity* **9**, 239–246 (1998).
19. Sheets, E. D., Holowka, D. & Baird, B. Critical role for cholesterol in Lyn-mediated tyrosine phosphorylation of FcεRI and their association with detergent-resistant membranes. *J. Cell Biol.* **145**, 877–887 (1999).
20. Anderson, S. J. & Perlmutter, R. M. A signaling pathway governing early thymocyte maturation. *Immunol. Today* **16**, 99–105 (1995).
21. Monks, C. R., Freiberg, B. A., Kupfer, H., Sciaky, N. & Kupfer, A. Three-dimensional segregation of supramolecular activation clusters in T cells. *Nature* **395**, 82–86 (1998).
22. Brown, D. A. & London, E. Functions of lipid rafts in biological membranes. *Annu. Rev. Cell Dev. Biol.* **14**, 111–136 (1998).
23. Lanzavecchia, A., Lezzi, G. & Viola, A. From TCR engagement to T cell activation: a kinetic view of T cell behavior. *Cell* **96**, 1–4 (1999).
24. Del Porto, P., Bruno, L., Mattei, M. G., von Boehmer, H. & Saint-Ruf, C. Cloning and comparative analysis of the human pre-T-cell receptor α-chain gene. *Proc. Natl Acad. Sci. USA* **92**, 12105–12109 (1995).
25. van Oers, N. S., von Boehmer, H. & Weiss, A. The pre-T cell receptor (TCR) complex is functionally coupled to the TCR-ζ subunit. *J. Exp. Med.* **182**, 1585-1590 (1995).
26. Wange, R. L., Malek, S. N., Desiderio, S. & Samelson, L. E. Tandem SH2 domains of ZAP-70 bind to T cell antigen receptor ζ and CD3ε from activated Jurkat T cells. *J. Biol. Chem.* **268**, 19797–19801 (1993).
27. Huby, R. D. J., Iwashima, M., Weiss, A. & Ley, S. C. ZAP-70 protein tyrosine kinase is constitutively targeted to the T cell cortex independently of its SH2 domains. *J. Cell Biol.* **137**, 1639–1649 (1997).
28. Irving, B. A., Alt, F. W. & Killeen, N. Thymocyte development in the absence of pre-T cell receptor extracellular immunoglobulin domains. *Science* **280**, 905–908 (1998).
29. Gunning, P., Leavitt, J., Muscat, G., Ng, S. Y. & Kedes, L. A human β-actin expression vector system directs high-level accumulation of antisense transcripts. *Proc. Natl Acad. Sci. USA* **84**, 4831–4835 (1987).

··

Distinct β-catenins mediate adhesion and signalling functions in *C. elegans*

Hendrik C. Korswagen*, Michael A. Herman† & Hans C. Clevers*‡

* *Department of Immunology and ‡ Center for Biomedical Genetics, University Medical Center Utrecht, Heidelberglaan 100, 3584 CX Utrecht, The Netherlands*
† *Program in Molecular, Cellular and Developmental Biology, Division of Biology, Kansas State University, Manhattan, Kansas 66506, USA*

··

In flies and vertebrates, Armadillo/β-catenin forms a complex with Tcf/Lef-1 transcription factors, serving as an essential co-activator to mediate Wnt signalling. It also associates with cadherins to mediate adhesion. In *Caenorhabditis elegans*, three putative β-catenin homologues have been identified: WRM-1, BAR-1 and HMP-2. WRM-1 and the Tcf homologue POP-1 mediate Wnt signalling by a mechanism that has challenged current views of the Wnt pathway[1–3]. Here we show that BAR-1 is the only β-catenin homologue that interacts directly with POP-1. BAR-1 mediates Wnt signalling by forming a BAR-1/POP-1 bipartite transcription factor that activates expression of Wnt target genes such as the Hox gene *mab-5*. HMP-2 is the only β-catenin homologue that interacts with the single cadherin of *C. elegans*, HMR-1. We conclude that a canonical Wnt pathway exists in *C. elegans*. Furthermore, our analysis shows that the functions of *C. elegans* β-catenins in adhesion and in signalling are performed by separate proteins.